PHILOSOPHICAL TRANSACTIONS OF THE ROYAL SOCIETY A

rsta.royalsocietypublishing.org

Review

Cite this article: Mali KS, De Feyter S. 2013 Principles of molecular assemblies leading to molecular nanostructures. Phil Trans R Soc A 371: 20120304.
http://dx.doi.org/10.1098/rsta.2012.0304

One contribution of 17 to a Theme Issue 'Molecular nanostructure and nanotechnology'.

Subject Areas:
supramolecular chemistry

Keywords:
self-assembly, molecular nanostructures, non-covalent interactions, monolayers, scanning tunnelling microscopy

Author for correspondence:
Steven De Feyter
e-mail: steven.defeyter@chem.kuleuven.be

Royal Society Publishing
Informing the science of the future

Principles of molecular assemblies leading to molecular nanostructures

Kunal S. Mali and Steven De Feyter

Division of Molecular Imaging and Photonics, Department of Chemistry, KU Leuven-University of Leuven, Celestijnenlaan, 200 F, 3001 Leuven, Belgium

Self-assembled physisorbed monolayers consist of regular two-dimensional arrays of molecules. Two-dimensional self-assembly of organic and metal–organic building blocks is a widely used strategy for nanoscale functionalization of surfaces. These supramolecular nanostructures are typically sustained by weak non-covalent forces such as van der Waals, electrostatic, metal–ligand, dipole–dipole and hydrogen bonding interactions. A wide variety of structurally very diverse monolayers have been fabricated under ambient conditions at the liquid–solid and air–solid interface or under ultra-high-vacuum (UHV) conditions at the UHV–solid interface. The outcome of the molecular self-assembly process depends on a variety of factors such as the nature of functional groups present on assembling molecules, the type of solvent, the temperature at which the molecules assemble and the concentration of the building blocks. The objective of this review is to provide a brief account of the progress in understanding various parameters affecting two-dimensional molecular self-assembly through illustration of some key examples from contemporary literature.

1. Introduction

Molecular synthesis, which constitutes a sizeable part of chemistry, is usually considered in the context of breaking and making of covalent bonds between atoms and molecules. On the other hand, relatively weaker non-covalent interactions, such as van der Waals forces, hydrogen bonds, π–π stacking, electrostatic and dipole–dipole interactions, can collectively be equally strong and play an important role in determining various material properties. These interactions have been used

in Nature for building complex supramolecular architectures via the process of biorecognition and biomolecular organization. Taking inspiration from Mother Nature, researchers have already begun to fabricate complex self-assembled architectures in which individual components interact via non-covalent forces. Described as the 'chemistry beyond the molecules' [1,2], this field has already permeated through most of chemistry and extended to the diverse array of other disciplines, including biology, physics, materials science and engineering.

Molecular self-assembly has been recognized as a very promising strategy for controlled bottom-up fabrication of functional nanostructures with tailor-made properties. The process of molecular self-assembly in solution has been extensively studied over the years and has contributed significantly to the general understanding of supramolecular interactions [3]. In contrast to their solution-phase assembly, assembling molecules on solid surfaces imparts a high degree of coherence in their alignment and packing, leading to well-defined two-dimensional nanostructures. Such surface-confined molecular layers can be used for nanoscale functionalization of surfaces with potential applications in diverse domains of science and technology. However, despite a myriad of investigations carried out since the seminal work of Foster & Frommer [4] and Rabe & Buchholz [5,6], most of the early findings on molecular self-assembly on surfaces were serendipitous. This is because the intermolecular interactions involved in the process are usually numerous, subtle, cooperative, multifaceted and have very little directionality (with the exception of hydrogen bonding). To explore the real potential of this approach, it is imperative to develop a clearer understanding of the various parameters that govern self-assembled network formation on surfaces. The present review discusses the principles of two-dimensional molecular self-assembly leading to the formation of well-defined arrays of molecules on surfaces as observed by scanning tunnelling microscopy (STM) [7]. The immensely popular class of chemisorbed self-assembled monolayers [8] (SAMs; for example, alkyl thiols on gold) is not discussed.

STM has been the method of choice for visualization as well as manipulation of these molecular layers in detail [9–14]. It allows imaging of these thin molecular layers adsorbed on atomically flat conductive substrates such as highly oriented pyrolytic graphite (HOPG) and Au(111) with submolecular resolution. A wide variety of structurally very diverse monolayers have been reported ranging from simple lamellar patterns to hierarchically structured complex multi-component systems. A vast majority of these studies deal with the structural aspects of monolayers and revolve around construction of two-dimensional supramolecular networks in a pre-programmed fashion. Just as in three dimensions, crystal engineering in two dimensions deals with elements of the well-known repertoire of non-covalent interactions that define supramolecular chemistry. The term 'two-dimensional crystal engineering' [15–22] has become increasingly recognized in recent years. One of the most extensively investigated facets is the structural polymorphism in these so-called two-dimensional crystals, wherein two different crystalline packings can be obtained upon deposition of a single building block. A number of experimental parameters have already been identified that control the appearance of a certain type of polymorph over another. A non-comprehensive list of these parameters includes the type of solvent [23–29], the concentration of molecules [30–35], the type of substrate [36–41], the temperature at which the self-assembly takes place [42–45] and the thermal history of the sample [46]. How these parameters affect the self-assembly of organic building blocks is the subject of this review, with a special focus on the liquid–solid interface.

2. Basics of molecular self-assembly on surfaces

The complexity of surface-confined molecular assembly process stems from the inherent intricacy of the adsorption process itself. The basic mechanism of all bottom-up fabrication strategies is that they essentially represent one or the other type of growth phenomenon. Typically, molecules are deposited onto a surface and, through a variety of processes involving intermolecular and interfacial interactions, nanometre-scale structures evolve. This phenomenon is a non-equilibrium process by default and is governed by a competition between kinetic and thermodynamic factors.

These factors differ significantly when self-assembled network formation under UHV conditions is considered against that at the liquid–solid interface. Adsorption at the liquid–solid interface is complicated by the presence of the supernatant liquid (typically an organic solvent) phase as well as the free exchange between the molecules adsorbed on the surface with those present in the liquid (solution) phase. Thus, apart from the intermolecular and molecule–substrate interactions, molecule–solvent and solvent–substrate interactions play a crucial role at the liquid–solid interface. In the absence of solvent, the complexity of the adsorption process is significantly reduced when molecules assemble at the UHV–solid interface [47,48].

Self-assembly on surfaces is primarily governed by a delicate balance between intermolecular and interfacial interactions. At room temperature, most low molecular weight organic compounds are too mobile and adsorption is favoured only when their adsorption energy (E_{ads}) is higher than their kinetic energy (E_{kin}). Interactions between adsorbed molecules are also crucial for the evolution of ordered networks. Intermolecular interactions should be strong enough to trap the molecules in a two-dimensional matrix, yet sufficiently reversible so that they allow for repair of defects. If the intermolecular interactions are too strong then the molecules 'stick' to each other irreversibly, preventing the formation of an ordered equilibrium structure. This condition necessitates that the intermolecular interaction energy (E_{int}) is only slightly higher than E_{kin}. In addition to the aforementioned energy considerations, the surface diffusion barriers (E_{dif}) of the molecules on a given surface are also very crucial. The optimal relationship between various energies relevant to the surface self-assembly process thus can be given as: $E_b > E_{inter} \geq E_{kin} > E_{dif}$. Whether the adsorption of molecules leads to the formation of a kinetically trapped metastable or thermodynamically stable equilibrium structure is governed by how quickly the molecules adsorb and how fast they move on the surface. If the rate of adsorption is faster than the surface diffusion rate, then molecules are not able to reach the equilibrium structure and are trapped in a diffusion-limited state. On the other hand, if the adsorption rate is slower or comparable to that of surface diffusion, then such a process leads to a thermodynamically favoured equilibrium structure [47,48].

The liquid–solid interface provides an experimentally simple alternative to self-assembly at the UHV–solid interface. However, as mentioned before, self-assembly at the liquid–solid interface is complicated by the presence of a third component, namely the solvent, which acts as a reservoir of molecules. The choice of solvent affects the mobility of molecules, especially the adsorption–desorption dynamics via the solvation energy and possibly also via the solvent viscosity. Once a drop of solution is applied onto a substrate, the dissolved species can diffuse towards the substrate, adsorb, diffuse laterally and desorb. The monolayer is thus in a dynamic equilibrium with the dissolved molecules in solution and constant adsorption–desorption is likely to prevail on time scales relevant for typical STM experiments [49]. This spontaneous dynamics is considered to be one of the main advantages of molecular self-assembly at the liquid–solid interface, because it favours the repair of defects. Thus, it was generally believed that self-assembly at the liquid–solid interface warrants the optimum conditions to achieve equilibrium and hence leads to formation of thermodynamically stable structures. However, there is increasing evidence that some of the two-dimensional molecular networks formed at the liquid–solid interface are in fact kinetically trapped structures and may not represent the minimum energy equilibrated state [46].

3. Role of the substrate and the medium

Despite their relatively weak nature, the molecule–substrate interactions have a strong bearing on the adsorption of molecules [36–41]. Detailed experimental and theoretical studies have revealed that the tendency of molecules in a two-dimensional monolayer to comply with the registry of the substrate lattice can result in significant changes in intermolecular interactions when compared with their self-assembly in three-dimensional crystals [36]. A wide range of atomically flat metal and semiconductor surfaces can be used under UHV conditions; however, many of them are not stable under ambient conditions. Therefore, HOPG has been

a substrate of choice, although other substrates such as Au(111), MoS_2 and $MoSe_2$ are also used under ambient conditions. The popularity of HOPG for such studies stems from the fact that it is inert, easy to clean and very stable under ambient conditions. Apart from these advantages, graphite also has a specific epitaxial interaction with alkyl chains which arises owing to the similarity between the zig-zag alternation of methylene groups and the [100] direction of the graphite lattice. Moreover, alkyl chains are stabilized by interchain interactions (interdigitation) wherein they stack laterally at a distance of approximately 4.1 Å [50]. This registry condition implies that, upon deposition, alkylated compounds search for the most favourable adsorption site on the HOPG surface such that the molecule–substrate and molecule–molecule van der Waals interactions are maximized.

Comparative studies describing the adsorption of a single building block on two different substrates are relatively scarce [51]. Nevertheless, one readily expects that the substrate lattice and thus the registry effects will be different for different substrates, which implies that the strength of molecule–substrate interactions will also be different. This influences the mobility of adsorbing species, which subsequently affects their ability to act as nucleation sites for growth of the network. Apart from simple, single-component systems, substrate effects also play a pivotal role in the formation of complex multi-component supramolecular networks, as illustrated by a comparative study of a three-component network carried out on Au(111) and HOPG [40].

Alkoxylated dehydrobenzo[12]annulene (DBA) derivatives (figure 1*a*) form honeycomb porous networks which are stabilized by van der Waals interactions between interdigitated pairs of alkyl chains. The rim of each hexagonal nanowell consists of a pair of alkyl chains from one DBA molecule, interdigitated with a pair from an adjacent molecule. When adsorbed on a surface, this interdigitation becomes chiral with two distinct interdigitation motifs, labelled arbitrarily (−) and (+) (figure 1*b*). The combination of interdigitation motifs within an individual nanowell can produce either chiral or achiral nanowells. Chiral nanowells have a combination of six identical interdigitation motifs. A chiral nanowell with all (−)-type interdigitation motifs leads to the formation of a so-called counterclockwise (CCW) nanowell, whereas the one with all (+)-type interdigitation motifs forms the clockwise (CW) nanowell (figure 1*b*) [52]. In the absence of any chiral influence, DBA on HOPG forms networks with equal amounts of domains containing CCW and CW nanowells, and the chirality of the nanowells is domain specific [15]. Achiral pores, on the other hand, have a combination of three (−)- and three (+)-type interdigitation motifs arranged in an alternating pattern (figure 1*b*).

Varying the alkyl chain length of DBA allows the pore size to be tuned to trap specific guest molecules or clusters to form multi-component systems. The nanowells formed by DBA with dodecyloxy chains can trap a heterocluster formed by one coronene (COR) and six isophthalic acid (ISA) molecules. The self-assembly of this multi-component system at the liquid–solid interface between Au(111) or HOPG and organic solvents results in different types of supramolecular networks. On Au(111) substrates, multi-component networks display an ordered superlattice arrangement of chiral and achiral pores (figure 1*c*,*e*). In comparison, similar networks on HOPG display only chiral pores (figure 1*d*,*f*) [15]. The unique superlattice structure observed on Au(111) could be related to a lower energetic preference for chiral pores than on HOPG and increased diffusion barriers for guest molecules. The increased diffusion barriers for guests allow them to act as nucleation sites for the formation of achiral pores. Following the initial nucleation of an achiral pore, restrictions imposed by the accommodation of guests within the porous network mean that subsequent growth naturally leads to the formation of the superlattice structure [40].

The medium from which the molecules adsorb on the surface is another fundamental parameter that can significantly influence the molecular organization on substrates. It strongly determines the deposition conditions and the related thermodynamic or kinetic parameters of the self-assembly process. Under UHV conditions, molecules are generally evaporated or alternatively a solution of them is sprayed onto the substrate by using a spray valve. A key advantage of working under UHV conditions is that one can obtain superior control over the surface coverage as well as temperature. Moreover, by using low and high temperatures, one can address kinetically trapped and thermodynamically equilibrated structures, respectively.

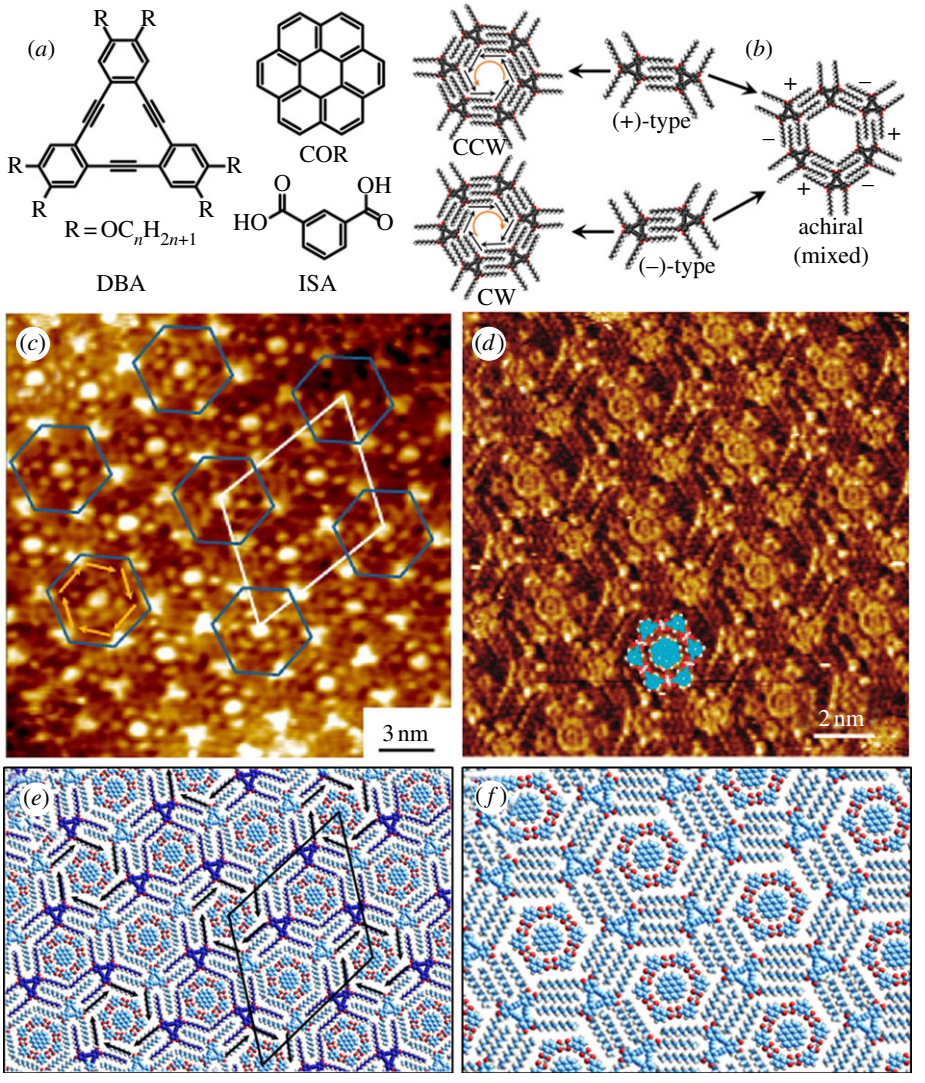

Figure 1. Substrate dependence of complex multi-component supramolecular networks. (*a*) Molecular structures of DBA, coronene and isophthalic acid. (*b*) Molecular models depicting the (+)- and (−)-type interdigitation patterns leading to the formation of chiral CCW and CW nanowells, respectively. A combination of three (+)-type and three (−)-type interdigitation patterns yields an achiral pore. (*c*) Three-component network formed at the 1-octanoic acid/Au(111) interface along with the molecular model (*e*). (*d*) Three-component network formed at the 1-octanoic acid/HOPG interface. Only chiral nanowells are formed. (*f*) Molecular model for the network formed on HOPG. (*c*,*e*) and (*d*) have been reproduced from references [40] and [15], respectively, with permission from the American Chemical Society. (Online version in colour.)

The presence of a vacuum above the monolayers does not limit the temperatures accessible for inducing (or reducing) dynamics when compared with monolayers formed at the liquid–solid interface where the presence of organic solvents restricts the annealing conditions. However, owing to its simplicity, the liquid–solid interface has gained immense popularity to assemble molecules in two dimensions.

The solvents used in STM studies at the liquid–solid interface are often chosen for practical reasons: they should dissolve the molecules of interest but not compete with them for surface adsorption, they should be chemically inert and they should have a low vapour pressure. Despite numerous investigations, the role of solvents in molecular self-assembly at the liquid–solid interface is less clearly understood. In the most ‘active’ mode of participation, the solvent

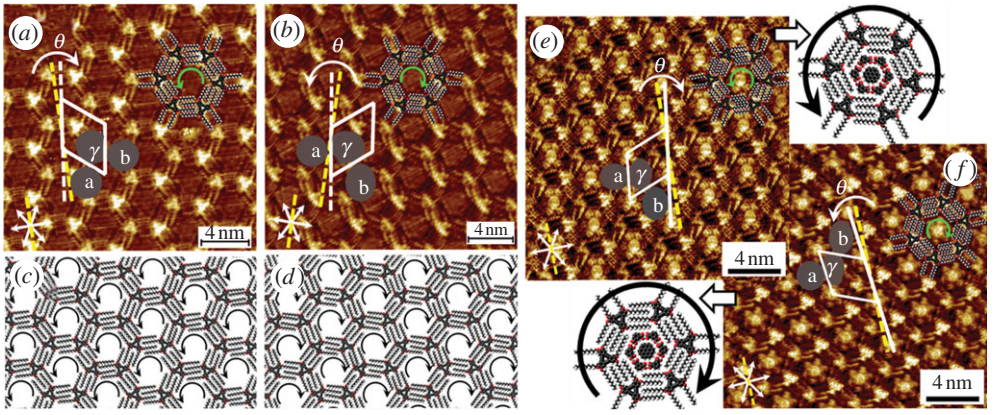

Figure 2. Solvent-induced homochirality in mono- and multi-component networks obtained at the interface between enantiopure 2-octanols and HOPG. (*a*) CCW honeycomb motif formed preferentially at the (*S*)-2-octanol/HOPG interface. (*b*) CW honeycomb motif formed preferentially at the (*R*)-2-octanol/HOPG interface. Molecular models shown in (*c*,*d*) reproduce the molecular packing in (*a*,*b*), respectively. (*e*,*f*) Homochiral three-component supramolecular networks consisting of COR–ISA6 heteroclusters trapped by voids of DBA host networks formed from (*S*)-2-octanol and (*R*)-2-octanol, respectively. Adapted from reference [23] with permission from the American Chemical Society. (Online version in colour.)

molecules undergo co-adsorption with the adsorbate molecules to form a multi-component monolayer. Solvent-induced polymorphism, the effect of co-adsorption as well as the solvent effects on electronic structures have been summarized recently [27].

In addition to their role as dispersing media, chiral enantiopure solvents can influence the handedness of the molecular networks formed at the liquid–solid interface [23,29]. The self-assembly of achiral DBA derivatives at the interface between enantiopure 2-octanol and HOPG resulted in the formation of homochiral monolayers in which the handedness of the porous supramolecular networks was determined by the handedness of the solvent. Self-assembly of DBA derivatives at the (*S*)-2-octanol/HOPG interface led to preferential formation of the (+)-type interdigitation pattern and thus the CCW honeycomb motif (figure 2*a*,*c*). On the other hand, (*R*)-2-octanol induced a clear bias towards preferential formation of the (−)-type interdigitation pattern and hence the CW honeycomb motif (figure 2*b*,*d*). The solvent-induced homochirality in these monolayers could also be discerned from the preferred orientations of the DBA networks with respect to the normal to the HOPG symmetry axis [23].

The assembly process consisted of recognition between a particular handed solvent molecule and the specific type of interdigitation pattern during the early stages of nucleation. A notable aspect of this solvent-mediated chirality transfer experiment was that the homochiral porous networks preserved their handedness even when the voids were occupied by guest clusters of COR and ISA (figure 2*e*,*f*). Thus, it is possible to store chiral information in the structure of the solvent molecules and then this information can be transferred to the multi-component supramolecular networks formed at the interface between such chiral solvents and an achiral substrate [23].

4. Role of concentration

When studying two-dimensional assembly at the liquid–solid interface, the number of molecules adsorbed at the interface as well as those present in the supernatant solution is extremely crucial and can be controlled by manipulating the solute concentration. Careful control over concentration can aid in selecting a specific structure, especially when two or more polymorphs are possible that differ in packing density or adsorption energy [30–35]. One of the first examples of concentration-dependent self-assembly was discovered in the case of alkoxylated DBA derivatives [30].

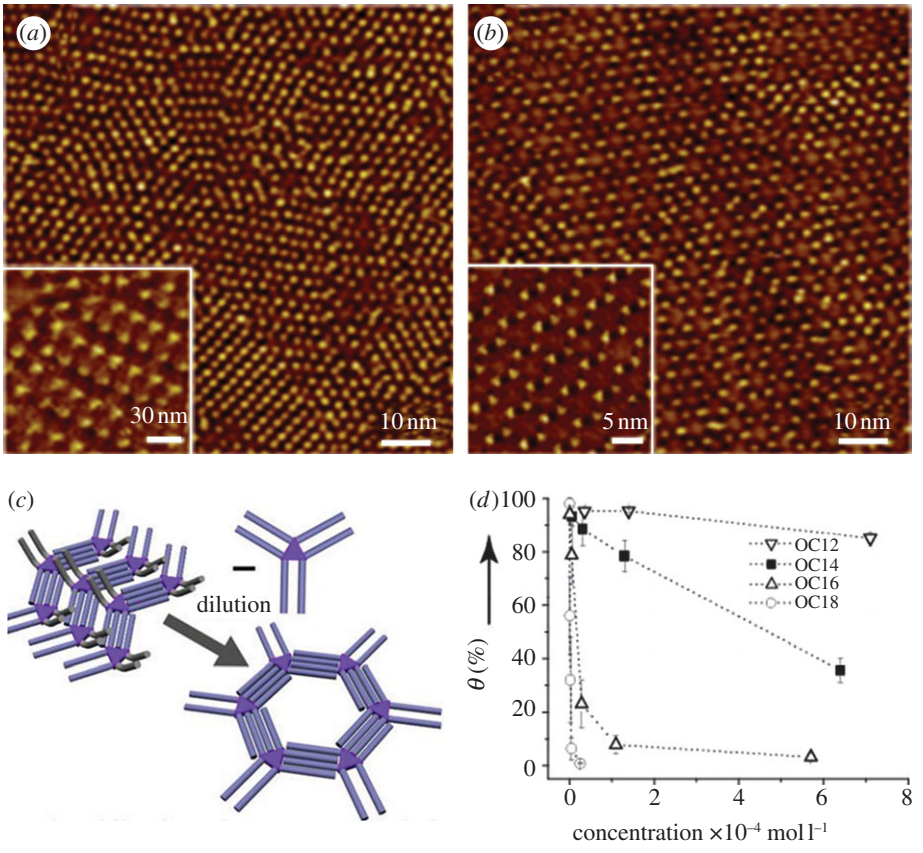

Figure 3. Concentration-controlled polymorphism in the monolayers of DBA–OC16 at the TCB/HOPG interface. (*a*,*b*) The high-density linear and low-density honeycomb networks obtained using high and low concentrations of DBA–OC16, respectively. The insets show magnified regions of STM images. (*c*) Schematic illustration of the linear to porous transition. (*d*) Dependence of surface coverage of the honeycomb pattern (θ) on the DBA concentration for different DBA derivatives. (*a*,*b*,*d*) Adapted from reference [30] with permission from Wiley-VCH. (Online version in colour.)

When the solution concentration is relatively high, DBA derivatives form a high-density linear packing, whereas at relatively lower concentrations, low-density nanoporous networks are obtained. Both polymorphs coexist at intermediate concentrations. The relative coverage of each polymorph thus could be controlled by meticulous choice of solution concentration. The STM images displayed in figure 3 clearly illustrate the concentration-dependent surface coverage of the linear and porous honeycomb networks for a DBA–OC16 derivative. A systematic examination of the concentration-dependent self-assembly of DBA derivatives with different alkoxy chain lengths, however, revealed that the concentration range in which this transformation is observed depends on the alkyl chain length. The surface coverage of the honeycomb network follows a linear relation with concentration for DBA derivatives with smaller alkoxy chains, whereas for DBA derivatives with longer alkoxy chains this relation is exponential (figure 3*d*) [30].

To further understand the mechanism of concentration-controlled structure selection of DBA derivatives at the liquid–solid interface, a thermodynamic model [30] was proposed which describes how the relative surface coverage correlates with concentration and temperature. Assuming that there exists an equilibrium between the molecules adsorbed in two polymorphs and the molecules present in solution, at full surface coverage, a measure of the relative coverage of the two polymorphs can be expressed as

$$\frac{Y_h}{Y_l^{(l/h)}} = \mathrm{e}^{((\mu_{0,\mathrm{solution}}-\mu_{0,\mathrm{h}})-(l/h)(\mu_{0,\mathrm{solution}}-\mu_{0,\mathrm{l}})/k_\mathrm{B}T)}c^{(1-l/h)}, \tag{4.1}$$

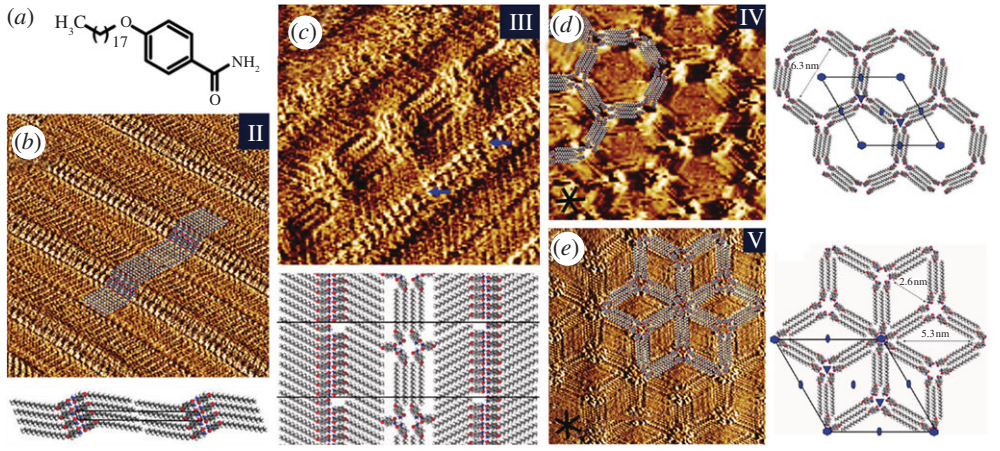

Figure 4. Concentration-controlled polymorphism in the monolayers of a C18 amide at the 1-phenyloctane/HOPG interface. (*a*) Molecular structure of C18 amide. (*b*,*c*) Close-packed structures obtained from relatively concentrated solutions. (*d*,*e*) Low-density nanoporous networks formed at relatively lower concentrations. Molecular models reproducing the packing of molecules in respective monolayers are also given near the STM images. Adapted from reference [34] with permission from the American Chemical Society. (Online version in colour.)

where Y_h and Y_l are the surface coverages of the honeycomb porous and linear networks, respectively, and h and l are the numbers of molecules per unit area in the respective pattern. $\mu_{0,\text{solution}}$, $\mu_{0,\text{h}}$ and $\mu_{0,\text{l}}$ are the chemical potentials of the molecules in solution, in the honeycomb and in the linear packing, respectively. This expression reproduces the experimental trend and describes how lowering the concentration c results in an increase in the ratio of the surface coverage of the honeycomb versus linear network. The two variables in equation (4.1), namely concentration c and temperature T, can thus be used to tune the relative surface coverage of the different polymorphs. The nature of the solvent is reflected in the chemical potential term $\mu_{0,\text{solution}}$, which is related to the solvation enthalpy, whereas $\mu_{0,\text{h}}$, and $\mu_{0,\text{l}}$ are characteristic for different adsorbates and their adsorption geometries on the surface and are related to adsorption enthalpy. As derivation of equation (4.1) is general and independent of the choice of adsorbate, solvent or substrate, it should in principle hold for all self-assembling systems in which one component can assemble into two different polymorphs [30].

The *concentration-in-control* principle has since been confirmed by various other studies [31–35]. The concentration effects, however, are not limited to high-symmetry molecules. Ahn & Matzger [34] demonstrated that a low-symmetry amide amphiphile can overcome geometric barriers to build highly symmetric monolayers using the concentration control strategy. For an amide with an octadecyloxy chain (figure 4*a*) adsorbed at the 1-phenyloctane/HOPG interface, they could observe as many as four different polymorphs with varying stabilities and densities. At relatively high concentrations (1.0×10^{-4} M), phase II is the major polymorph (figure 4*b*) along with phase III which appears as a minor structure (figure 4*c*). Upon reducing the concentration, within a concentration range of 3.3×10^{-5} M to 5.0×10^{-4} M, two different types of nanoporous networks were visualized—namely, a rhombic nanoporous network (figure 4*d*) and a honeycomb porous network (figure 4*e*). The rhombic network is the preferred polymorph formed from dilute solutions. As this bonding pattern is kinetically not easily accessible, polymorph IV is formed initially, which transforms into thermodynamically favoured polymorph V.

The respective stabilities of these polymorphs at given concentrations were confirmed by changing the concentration *in situ* by addition of 1-phenyloctane. For example, when the concentration of solution was decreased by adding solvent, a gradual phase transformation from phase II to phase V via phase IV was observed. As at no concentration was phase IV

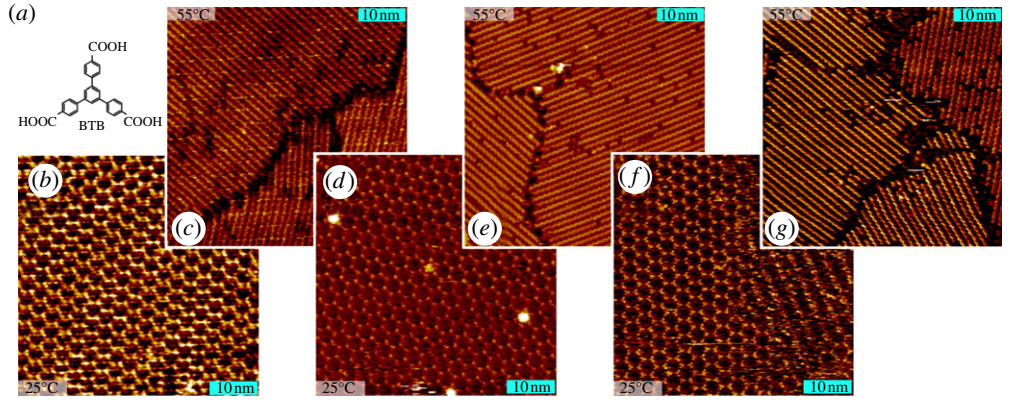

Figure 5. (*a*) Molecular structure of BTB. (*b–g*) Temperature-induced reversible phase transitions in the monolayers of BTB at the 1-nonanoic acid/HOPG interface. The respective temperatures are stated in the lower or upper left corner of each image. Adapted from reference [45] with permission from the American Chemical Society. (Online version in colour.)

observed as a stable polymorph, it was concluded that it is only kinetically accessible and not thermodynamically stable. In addition to its fundamental interest, the concentration dependence of self-assembly provides an elegant way of fabricating several energetically viable supramolecular aggregation patterns by simply manipulating the solute concentration [34].

5. Role of temperature and thermal history

It is apparent from equation (4.1) that, besides concentration, temperature is an essential parameter governing the self-assembly process as it affects both the thermodynamics as well as the kinetics of the system. Despite this fact, among all the important parameters critical to the self-assembly process, the temperature effect on the self-assembly at the liquid–solid interface is the least studied [42–45,53]. Although variable temperature experiments under UHV conditions are done routinely, very often samples are conditioned at elevated temperature, whereas the STM measurements are still carried out at room temperature or cryogenic temperatures.

In a recent study, Lackinger and co-workers [45] addressed the temperature dependence of molecular self-assembly at the liquid–solid interface by *in situ* STM visualization of temperature-induced phase transitions in the monolayers of 1,3,5-*tris*(4-carboxyphenyl)benzene (BTB) (figure 5*a*). Self-assembly of BTB at the 1-octanoic acid/HOPG interface, at room temperature, leads to emergence of two different polymorphs; namely, a high-density row structure (figure 5*c*) and a low-density porous structure (figure 5*b*). However, the high- and the low-density polymorphs could be obtained exclusively when the self-assembly is carried out from 1-heptanoic and 1-nonanoic acid, respectively. Heating the BTB/1-octanoic acid/HOPG system (where both polymorphs coexist) above 43°C leads to a phase transition wherein the entire surface gets covered with row structure. Similarly, the low-density porous polymorph formed at the 1-nonanoic acid/HOPG interface transforms into the high-density row structure above 55°C. These structural transitions could be induced reversibly by variation of temperature above and below the transition temperatures mentioned above [45].

Both of the polymorphs are assumed to be thermodynamically stable under given experimental conditions, and the reversibility of the transition process further confirms that the porous network obtained at relatively lower temperatures is not merely a kinetically trapped structure. Adsorption of molecules at the liquid–solid interface represents a trade-off between solvation and adsorption enthalpy. While a favourable adsorption enthalpy helps to minimize the Gibbs free energy, the accompanying loss of entropy upon adsorption acts against it. For this reason, the enthalpic and entropic contributions to the Gibbs free energy are important. A

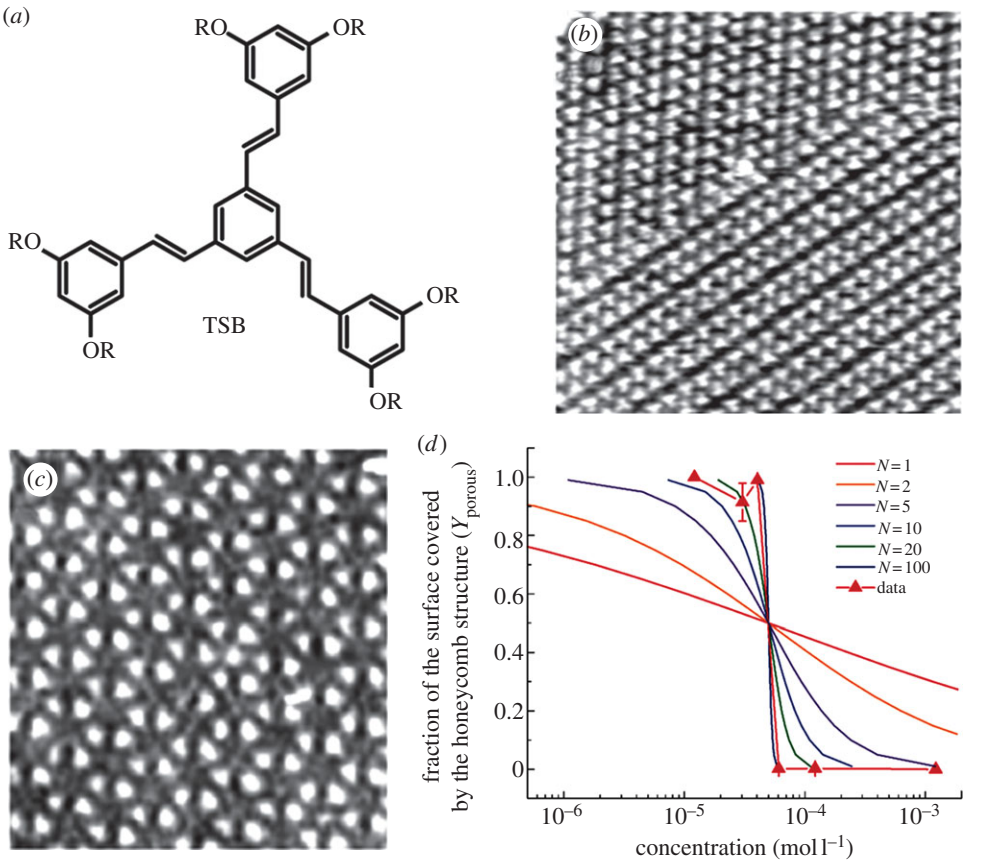

Figure 6. Influence of growth history on monolayers. (*a*) Molecular structure of TSB. (*b*) Monolayer of TSB obtained upon deposition of solution on HOPG held at lower temperature and then annealing at 60°C for 1 h. (*c*) Monolayer structure upon deposition onto HOPG held at 60°C followed by annealing at 60°C for 1 h. (*d*) A plot showing the fraction of the surface covered by the porous network as a function of concentration along with calculated curves. Adapted from reference [46] with permission from the American Institute of Physics. (Online version in colour.)

reduction in the degrees of freedom upon adsorption implies a reduction in the entropy, which increases the Gibbs free energy of the system. As a consequence, spontaneous self-assembly of molecular components necessitates that the loss of entropy at a given temperature must be compensated by gain in enthalpy upon adsorption. The authors used molecular mechanics calculations to compute binding enthalpies, whereas the changes in the entropy were estimated using a method proposed by Whitesides and co-workers [54]. The thermodynamic model developed using these estimates could be fully understood only when solvent coadsorption in the voids of the nanoporous networks was taken into account. Using this approach, they could quantitatively estimate the changes in Gibbs free energy for the two phases of BTB and also reproduced the experimental trend for phase transitions [45].

Charra and co-workers [46] demonstrated that not only the annealing temperatures but also the growth history of the sample is critical in the selection of a particular polymorph in an equilibrating system. Similar to the DBA derivatives discussed in previous sections, dodecyloxy substituted 1,3,5-tristyrylbenzene (TSB; figure 6*a*) self-assembles into a high-density linear (figure 6*b*) and a low-density honeycomb porous (figure 6*c*) polymorph at the 1-phenyloctane/HOPG interface. STM images recorded immediately after application of a droplet of TSB solution onto the HOPG substrate held at 21°C revealed only disordered aggregates. This system was then

allowed to equilibrate for 1 h, during which the substrate was held at 60°C. STM visualization of such a sample revealed the formation of large domains of densely packed polymorph. In the second experiment, the TSB droplet was applied onto HOPG held at 60°C and the temperature was held constant for 1 h. This led to the formation of large domains of porous molecular networks. These experiments demonstrate that, for a given final temperature and concentration, the characteristics of the adsorbed monolayer strongly depend on its growth history, that is, on the detailed sequence of temperatures applied during and after the solution droplet deposition. The authors assimilated these observations by considering different nucleation and growth rates for the two polymorphs and argued that, even at relatively high temperatures, a kinetic blockade prevents the transition of the thermodynamically less stable porous structure to the more stable high-density linear structure [46].

Temperature evolution of the percentage surface coverage for the honeycomb network of different TSB derivatives revealed that sharp phase transitions appear at precise concentrations. This observation is in contrast to the one made in the case of DBA derivatives, wherein the phase transitions were more gradual. The authors addressed this discrepancy by considering the equilibrium between molecules in solution and entire domains of the two polymorphs instead of independent molecules adsorbed in dense and porous domains. Thus, the thermodynamic model takes the form

$$\left[\frac{Y_h}{Y_l^{(l/h)}}\right]^{1/N} = \mathrm{e}^{((\mu_{0,\mathrm{solution}}-(1/N)\mu_{0,\mathrm{h}})-(l/h)(\mu_{0,\mathrm{solution}}-(1/N)\mu_{0,\mathrm{l}})/k_\mathrm{B}T)}c^{(1-l/h)}. \tag{5.1}$$

The factor $1/N$ in equation (5.1) is the only mathematical change compared with the expression given in equation (4.1). It is a dimensionless parameter in the redefined chemical potential term for two-dimensional aggregates of aggregation number N and accounts for molecular interactions responsible for domain formation instead of disordered aggregates. For $N = 1$, equation (5.1) reduces to equation (4.1). For larger values of N (for example, $N = 100$), this model could reproduce the sharp phase transitions observed by the authors (figure 6*d*) [46].

6. Dynamics and phase transitions in two-dimensional monolayers

It is clear from the discussion presented in previous sections that, apart from thermodynamics, kinetics too plays an important role in the self-assembly process. The dynamics during early nucleation events and also after the surface is covered with molecules determines whether the monolayer represents a kinetically trapped metastable or thermodynamically stable equilibrated state. Apart from the spontaneous dynamics inherent to each system, the movement of molecules can be induced by external stimuli such as light [55–57], interactions with the STM tip [58], changes in electrical potential [59], molecular additives [60–62] and, as discussed in the previous section, changes in temperature [42–45,53]. These dynamic phenomena assume special importance in the context of phase transitions in two-dimensional molecular systems.

Ernst and co-workers [63] reported temperature-controlled reversible phase transitions in the monolayers of bowl-shaped corannulene molecules at the UHV/Cu(111) interface. At room temperature, a regular array of molecules is formed (figure 7*e*). Reduction in the substrate temperature leads to two different phase transitions. A denser lattice is formed at 225 K (figure 7*f*), and it converts to another structure (figure 7*g*) upon further cooling of the substrate to around 69 K. These transitions are reversible, and it was possible to revert back to the room temperature phase via the intermediate phase upon heating the substrate. The subsequent phase transitions caused a 14.3% increase in the lattice density upon cooling the substrate.

The asymmetrical appearance of the molecules indicates that they are substantially tilted on the Cu(111) surface. Furthermore, from the comparison of the lattice parameters, the authors confirm that the intermediate phase is formed owing to the compression of molecules along one lattice direction. Cooling of the room temperature phase leads to wiggling motions of molecules in every alternate row (identified from different STM contrasts) and further leads to zipper-like

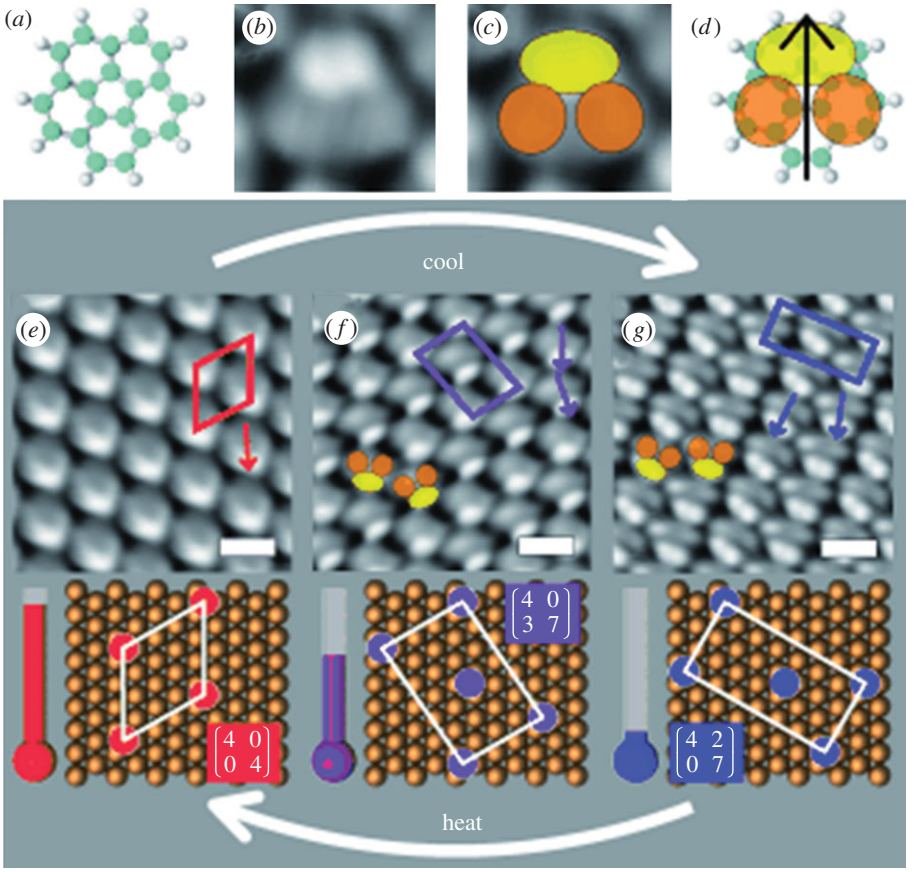

Figure 7. Reversible phase transitions in the monolayers of corannulene on Cu(111). (*a*) Ball and stick model of corannulene. (*b–d*) Correlation of the STM contrast with molecular structure, revealing a tilted adsorption geometry of molecules on the Cu(111) surface. (*e*) Room temperature phase. (*f*) Intermediate temperature phase formed at 225 K. (*g*) Low-temperature phase obtained upon further cooling to 69 K. Adapted from reference [63] with permission from Wiley-VCH. (Online version in colour.)

displacement of several adjacent molecules. The migration proceeds via the fcc to hcp threefold hollow sites of the copper lattice. The second transition does not involve any change in the lattice density but a mere rearrangement to adjust to the most favourable fcc threefold hollow site. The compression of molecular lattice was explained by considering the breathing mode vibrations of the molecules at room temperature, which require larger space on the substrate. Cooling of the system leads to suppression of these vibrational modes and thus decreases the spatial requirements of the molecules, enabling closer packing [63].

Molecular dynamics and thus phase transitions can also be induced by using light irradiation if the supramolecular network contains light responsive functional units. Azobenzene-based organic building blocks have often been used to extract reversible photoresponse [56,57] from molecular nanostructures. Gong and co-workers [55] exploited the photosensitive azobenzene groups to realize reversible phase transitions in a complex three-component system. The building block used consisted of a 4NN-macrocycle (figure 8*b*) containing four azobenzene units. This molecule could be immobilized by using a molecular template formed by TCDB molecules (figure 8*a*). The 4NN-macrocycle adsorbs with all its azobenzene units in the all-*trans* (t,t,t,t) conformation. Addition of COR to this two-component network does not lead to significant changes in the dimensions of the lattice parameters. COR molecules are not immobilized into the cavities of the 4NN-macrocycle but rather sit atop the monolayer (figure 8*e*) [55].

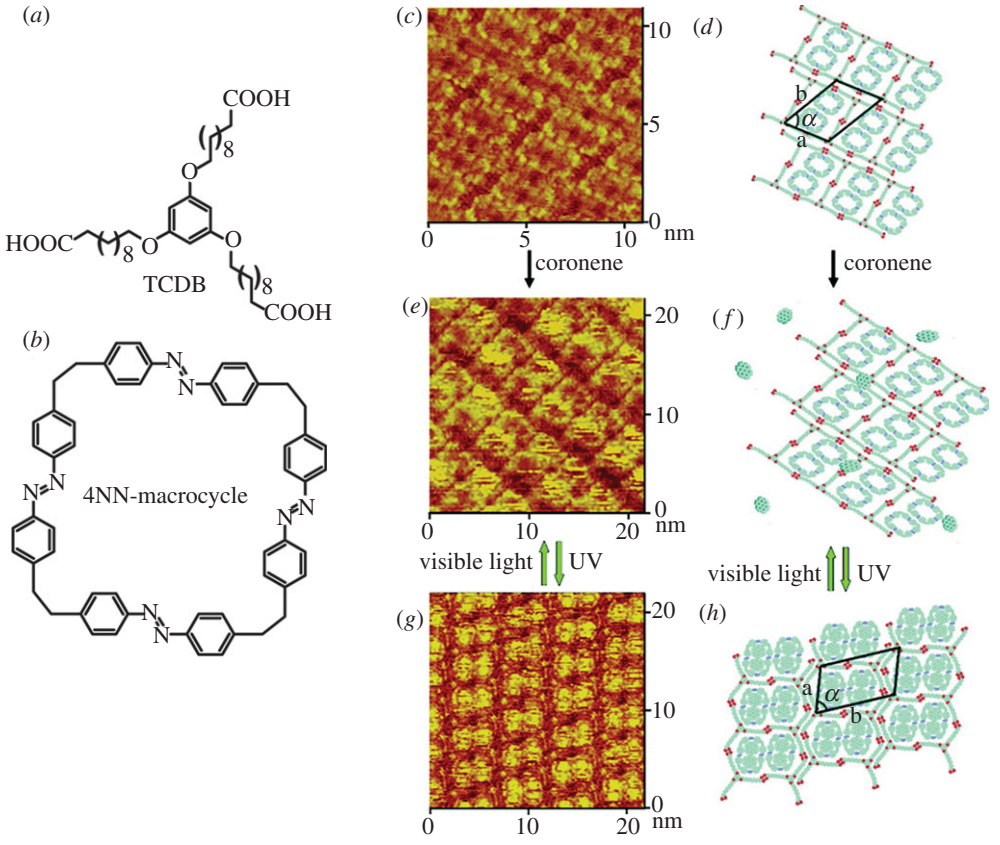

Figure 8. Photoswitchable ternary supramolecular network formed at the 1-heptanoic acid/HOPG interface. (*a*,*b*) Molecular structures of TCDB and the 4NN-macrocycle. (*c*,*d*) Two-component network consisting of TCDB and the 4NN-macrocycle. (*e*,*f*) The three-component system prior to UV irradiation. (*g*,*h*) The three-component system after UV irradiation. The immobilized coronene molecules could be visualized clearly. Adapted from reference [55] with permission from the American Chemical Society. (Online version in colour.)

Upon UV irradiation, a new supramolecular arrangement is observed in which the voids of the host network are occupied by immobilized COR molecules. The shape of the macrocycle changes from parallelogram to ellipsoidal after irradiation, and it is attributed to the photoinduced *trans* to *cis* isomerization of the two azobenzene units which transform the macrocycle from the (t,t,t,t) to the (t,c,t,c) conformation. This transformation increases the effective area of the voids and thus COR molecules are immobilized in the voids to form a well-ordered array of host–guest type network. The reverse process of the transformation of the *cis* conformation back to the more stable all-*trans* conformation is induced by irradiation with visible light, in which case the COR molecules are expelled from the pores owing to shrinkage of the porous voids. Such reversible phase transformations are central to the development of molecular-scale switches [55].

7. Thermodynamics of reactions and catalysis in two-dimensional monolayers

Temperature control of self-assembly provides valuable information concerning diffusion and reaction rates, activation energies and thermodynamic parameters such as the entropy and enthalpy of various processes including surface-supported reactions and catalysis. Although relatively nascent, an increasing number of researchers are addressing the thermodynamic and kinetic aspects of these processes. Such investigations are immensely important from a commercial point of view owing to their relevance to heterogeneous catalysis.

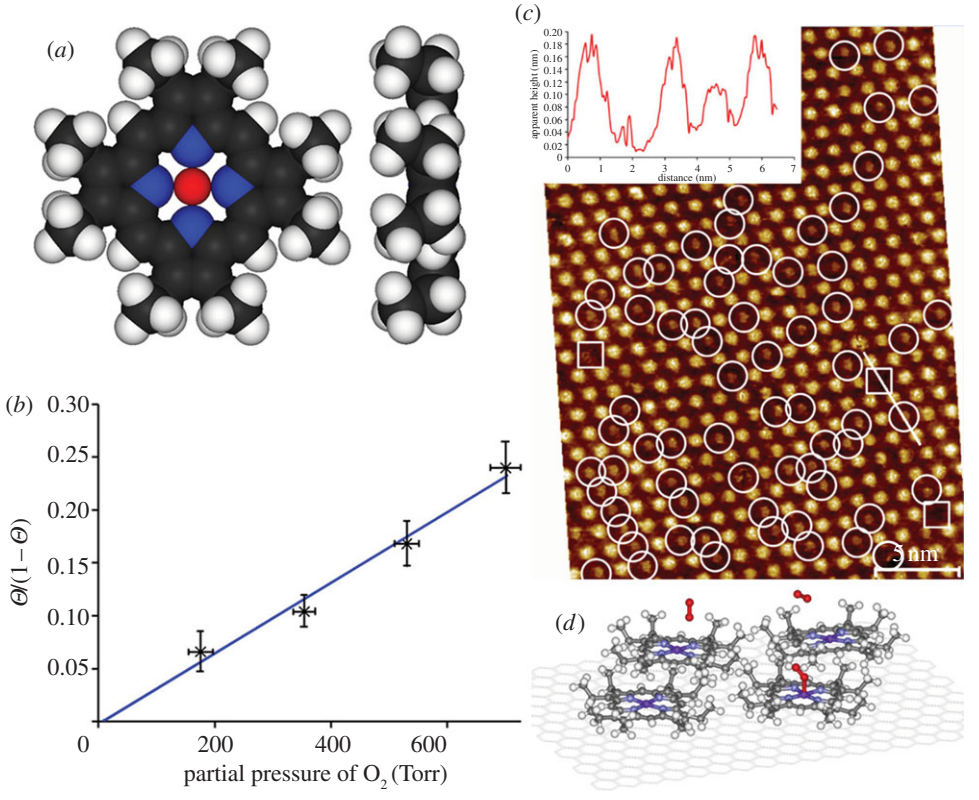

Figure 9. Oxygen binding of molecular oxygen to CoOEP at the liquid–solid interface. (*a*) Model for the CoOEP. (*b*) Plot of the relative surface coverage of oxygenated species against partial pressure of O_2. (*c*) STM image of CoOEP at the 1-phenyloctane–HOPG interface. White circles highlight the molecules with bound oxygen, whereas white squares show vacancies in the monolayer. (*d*) A schematic illustrating the oxygen-binding process on the HOPG surface. Adapted from reference [64] with permission from the American Chemical Society. (Online version in colour.)

In a recent study, Hipps and co-workers [64] studied the thermodynamics of the reversible binding of oxygen to cobalt (II) octaethylporphyrin (CoOEP; figure 9*a*) adsorbed at the 1-phenyloctane/HOPG interface. The monolayer of CoOEP adsorbed at 25°C in equilibrium with pure O_2 shows varying STM contrast (figure 9*c*). Some molecules appear brighter than others and the authors interpreted the darker features as molecules with axially bound O_2. An increase in the partial pressure of O_2 led to an increase in the number of dark molecules in the monolayer (figure 9*b*). The oxygen-binding process follows the Langmuir isotherm in which the relative surface coverage of dark molecules is proportional to the partial pressure of O_2. Using this plot, the authors calculated the equilibrium constant for O_2 adsorption, which was further used to calculate the free energy change for the binding process. By carrying out STM measurements at different temperatures and at 100% O_2 saturation, the authors obtained a plot of the free energy change versus the temperature, the slope of which corresponds to the entropy change of the process relative to the standard state. From this value of entropy, it was possible to calculate the enthalpy changes associated with the process [64].

Thus, all the thermodynamic parameters associated with the O_2-binding process could be obtained from STM measurements. The enthalpy and entropy changes were found to be larger than those reported for solution-phase experiments for the same process. The authors point out that room temperature binding of O_2 to CoOEP is generally impossible under solution conditions and it is made feasible owing to the adsorption of molecules on the HOPG surface. The stability of the bound oxygen was attributed to the charge donation from the graphite surface, which

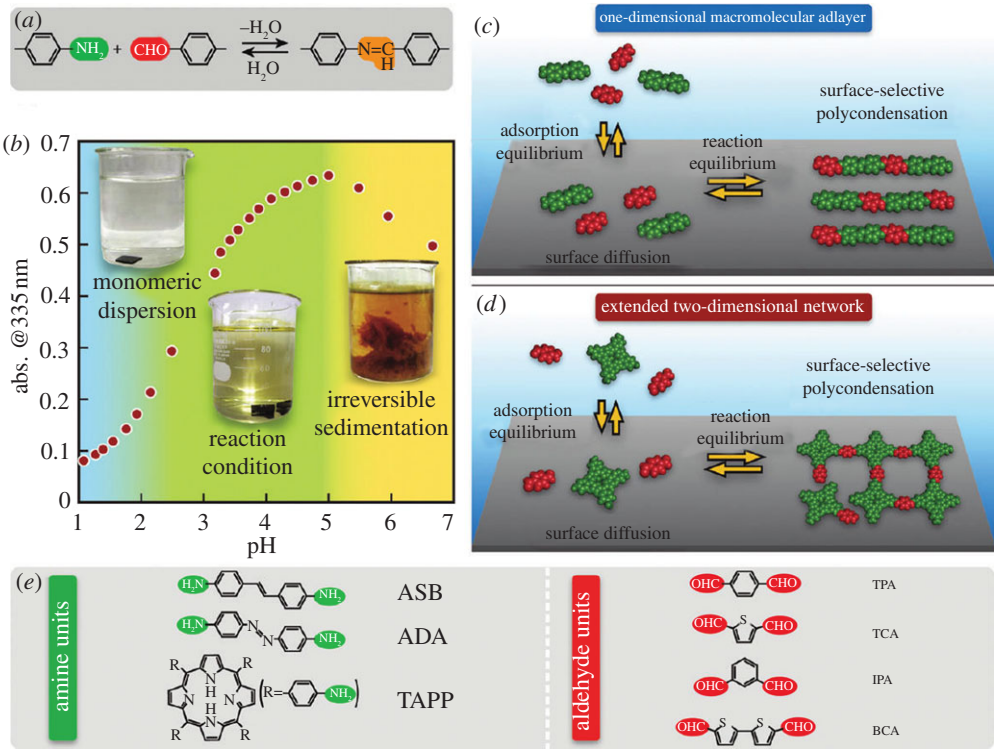

Figure 10. Thermodynamically controlled polycondensation reaction at the liquid–solid interface. (*a*) General reaction scheme. (*b*) pH-dependent absorbance of the solution containing a mixture of 4,4′-diaminostilbene dihydrochloride (ASB) and terephthaldicarboxaldehyde (TPA). (*c*,*d*) Schematic of the equilibrium processes leading to formation of extended one-dimensional and two-dimensional covalent networks, respectively. (*e*) Molecular building blocks used for the surface selective polycondensation reaction. Adapted from reference [68] with permission from the American Chemical Society. (Online version in colour.)

essentially acts as a fifth ligand [64]. The ability of a surface to act as an additional ligand for porphyrins was reported earlier by Elemans and co-workers [65] for alkylated Mn-porphyrin monolayers adsorbed at the tetradecane/Au(111) surface.

Recent years have witnessed a surge in reports describing surface-supported synthesis and STM of two-dimensional covalent networks [66–70]. Selective intermolecular interactions have been widely exploited to couple non-covalently assembled molecular components in a more ‘permanent’ covalent fashion. Initial attempts to synthesize such two-dimensional covalent organic frameworks (COFs) were limited to the UHV systems. In general, the UHV experiments used kinetically controlled, thermally activated reactions conducted at very low surface coverages in order to control the supply of molecular building blocks to prevent undesired side reactions. Kunitake and co-workers [68] provided a breakthrough in the much sought after ambient solution/solid interface synthesis of two-dimensional COFs recently by covalent linking of a series of aromatic aldehydes and amines. An advantage of such equilibrium-controlled covalent coupling is that it eliminates the necessity for severe conditions and sophisticated equipment.

Figure 10 shows the general concept of the covalent coupling methodology developed by the authors. It consists of an equilibrium polycondensation reaction between aromatic primary amines and aldehydes to form two-dimensional COFs. This reaction is reversible when carried out under mild aqueous solution conditions.

By exploring the thermodynamic control of the reaction conditions by carefully varying the pH of the system, they could successfully fabricate various π-conjugated polymers on an iodine-modified Au(111) substrate. The visualization of the two-dimensional COFs was carried out using

electrochemical STM. The reversibility of the reaction under given conditions coupled with the reversibility of the adsorption and non-covalent network formation at the liquid–solid interface led to formation of extended covalent networks under solution conditions. As the process is not limited to two-dimensional structures, it can be readily applied to arbitrary three-dimensional COFs as well.

8. Summary and outlook

A steadily growing number of researchers from diverse disciplines are exploring the opportunities brought forward by the research on molecular self-assembly. A common goal is the fabrication of supramolecular nanostructures in a controlled and reproducible manner. A prerequisite for achieving this goal is the precise understanding of the thermodynamic and kinetic parameters that govern the self-assembled network formation. Although many of the supramolecular interactions that exist in the three dimensions can be translated to build nanostructures in two dimensions, care must be taken when extending the concepts in three dimensions to two dimensions and vice versa because the presence of a substrate and solvent complicate the two-dimensional self-assembly process. For example, concentration-dependent polymorphism in crystal structures is alien to three-dimensional crystallizations, whereas it is routinely observed in the case of two-dimensional self-assembled monolayers.

A number of thermodynamic and kinetic models have been proposed to address phenomena that are unique to nanostructures formed at liquid–solid interfaces. Concentration- and temperature-dependent changes in two-dimensional nanostructures have been assimilated using such thermodynamic models. Despite the understanding developed so far, a number of parameters that are crucial to the self-assembly process at these interfaces lack a thorough theoretical and sometimes even experimental description. For example, the thermodynamic models that accommodate solvent-related parameters such as solvation enthalpy (related to the thermodynamics of the system) and viscosity (related to the diffusion rates and hence the kinetics of the system) have not been developed yet. An exciting development is the real-time and real-space exploration of chemical reactions and catalysis which can lead to unique covalently linked two-dimensional nanostructures. An increasing number of studies are addressing these issues, which will help in the development of more rational approaches for the fabrication of molecular nanostructures.

Acknowledgements. In particular, we thank the group of Prof. Tobe from Osaka University for very fruitful collaboration. In addition, Prof. Sheng-bin Lei from the Harbin Institute of Technology is acknowledged for his contribution.

Funding statement. This work is supported by KU Leuven through GOA 2006/2, Funding for Scientific Research—Flanders (F.W.O.) and the Belgian Federal Science Policy Office through IAP 7/05.

References

1. Lehn J-M. 1998 *Supramolecular chemistry*. Weinheim, Germany: Wiley-VCH.
2. Whitesides GM, Grzybowski B. 2002 Self-assembly at all scales. *Science* **295**, 2418–2421. (doi:10.1126/science.1070821)
3. Lehn J-M. 1990 Perspectives in supramolecular chemistry: from molecular recognition towards molecular information processing and self-organization. *Angew. Chem. Int. Ed.* **29**, 1304–1319. (doi:10.1002/anie.199013041)
4. Foster JS, Frommer JE. 1988 Imaging of liquid crystals using a tunnelling microscope. *Nature* **333**, 542–545. (doi:10.1038/333542a0)
5. Rabe JP, Buchholz S. 1991 Commensurability and mobility in two-dimensional molecular patterns on graphite. *Science* **253**, 424–427. (doi:10.1126/science.253.5018.424)
6. Rabe JP, Buchholz S. 1991 Direct observation of molecular structure and dynamics at the interface between a solid wall and an organic solution by scanning tunneling microscopy. *Phys. Rev. Lett.* **66**, 2096–2099. (doi:10.1103/PhysRevLett.66.2096)

7. De Feyter S, De Schryver FC. 2005 Self-assembly at the liquid/solid interface: STM reveals. *J. Phys. Chem. B* **109**, 4290–4302. (doi:10.1021/jp045298k)
8. Lewis PA, Donhauser ZJ, Mantooth BA, Smith RK, Bumm LA, Kelly KF, Weiss PS. 2001 Control and placement of molecules via self-assembly. *Nanotechnology* **12**, 231. (doi:10.1088/0957-4484/12/3/306)
9. Giancarlo LC, Flynn GW. 2000 Raising flags: applications of chemical marker groups to study self-assembly, chirality, and orientation of interfacial films by scanning tunneling microscopy. *Acc. Chem. Res.* **33**, 491–501. (doi:10.1021/ar970261m)
10. Otero R, Rosei F, Besenbacher F. 2006 Scanning tunneling microscopy manipulation of complex organic molecules on solid surfaces. *Annu. Rev. Phys. Chem.* **57**, 497–525. (doi:10.1146/annurev.physchem.57.032905.104634)
11. Wan L-J. 2006 Fabricating and controlling molecular self-organization at solid surfaces: studies by scanning tunneling microscopy. *Acc. Chem. Res.* **39**, 334–342. (doi:10.1021/ar0501929)
12. Yang Y, Wang C. 2009 Hierarchical construction of self-assembled low-dimensional molecular architectures observed by using scanning tunneling microscopy. *Chem. Soc. Rev.* **38**, 2576–2589. (doi:10.1039/b807500j)
13. Wu P, Zeng Q, Xu S, Wang C, Yin S, Bai C-L. 2001 Molecular superlattices induced by alkyl substitutions in self-assembled triphenylene monolayers. *Chemphyschem* **2**, 750–754. (doi:10.1002/1439–7641(20011217)2:12<750::AID-CPHC750>3.0.CO;2–9)
14. Qiu X, Wang C, Zeng Q, Xu B, Yin S, Wang H, Xu S, Bai C. 2000 Alkane-assisted adsorption and assembly of phthalocyanines and porphyrins. *J. Am. Chem. Soc.* **122**, 5550–5556. (doi:10.1021/ja994271p)
15. Lei S, Surin M, Tahara K, Adisoejoso J, Lazzaroni R, Tobe Y, De Feyter S. 2008 Programmable hierarchical three-component 2D assembly at a liquid-solid interface: recognition, selection, and transformation. *Nano Lett.* **8**, 2541–2546. (doi:10.1021/nl8016626)
16. Adisoejoso J, Tahara K, Okuhata S, Lei S, Tobe Y, De Feyter S. 2009 Two-dimensional crystal engineering: a four-component architecture at a liquid–solid interface. *Angew. Chem. Int. Ed.* **48**, 7353–7357. (doi:10.1002/anie.200900436)
17. Xue Y, Zimmt MB. 2012 Patterned monolayer self-assembly programmed by side chain shape: four-component gratings. *J. Am. Chem. Soc.* **134**, 4513–4516. (doi:10.1021/ja2115019)
18. Bertrand H, Silly F, Teulade-Fichou M-P, Tortech L, Fichou D. 2011 Locking the free-rotation of a prochiral star-shaped guest molecule inside a two-dimensional nanoporous network by introduction of chlorine atoms. *Chem. Commun.* **47**, 10 091–10 093. (doi:10.1039/c1cc12951a)
19. Miao X, Xu L, Li Y, Li Z, Zhou J, Deng W. 2010 Tuning the packing density of host molecular self-assemblies at the solid–liquid interface using guest molecule. *Chem. Commun.* **46**, 8830–8832. (doi:10.1039/c0cc02554b)
20. Shi Z, Lin T, Liu J, Liu PN, Lin N. 2011 Regulating a two-dimensional metallo-supramolecular self-assembly of multiple outputs. *CrystEngComm* **13**, 5532–5534. (doi:10.1039/c1ce05340j)
21. Piot L, Silly F, Tortech L, Nicolas Y, Blanchard P, Roncali J, Fichou D. 2009 Long-range alignments of single fullerenes by site-selective inclusion into a double-cavity 2D open network. *J. Am. Chem. Soc.* **131**, 12 864–12 865. (doi:10.1021/ja902621t)
22. Zhang HL, Chen W, Huang H, Chen L, Wee ATS. 2008 Preferential trapping of C_{60} in nanomesh voids. *J. Am. Chem. Soc.* **130**, 2720–2721. (doi:10.1021/ja710009q)
23. Destoop I, Ghijsens E, Katayama K, Tahara K, Mali KS, Tobe Y, De Feyter S. 2012 Solvent-induced homochirality in surface-confined low-density nanoporous molecular networks. *J. Am. Chem. Soc.* **134**, 19 568–19 571. (doi:10.1021/ja309673t)
24. Mamdouh W, Uji-I H, Ladislaw JS, Dulcey AE, Percec V, De Schryver FC, De Feyter S. 2005 Solvent controlled self-assembly at the liquid–solid interface revealed by STM. *J. Am. Chem. Soc.* **128**, 317–325. (doi:10.1021/ja056175w)
25. Lackinger M, Griessl S, Heckl WM, Hietschold M, Flynn GW. 2005 Self-assembly of trimesic acid at the liquid-solid interface: a study of solvent-induced polymorphism. *Langmuir* **21**, 4984–4988. (doi:10.1021/la0467640)
26. Nath KG, Ivasenko O, Miwa JA, Dang H, Wuest JD, Nanci A, Perepichka DF, Rosei F. 2006 Rational modulation of the periodicity in linear hydrogen-bonded assemblies of trimesic acid on surfaces. *J. Am. Chem. Soc.* **128**, 4212–4213. (doi:10.1021/ja0602896)
27. Yang Y, Wang C. 2009 Solvent effects on two-dimensional molecular self-assemblies investigated by using scanning tunneling microscopy. *Curr. Opin. Colloid Int.* **14**, 135–147. (doi:10.1016/j.cocis.2008.10.002)

28. Zhang X, Chen T, Chen Q, Deng G-J, Fan Q-H, Wan L-J. 2009 One solvent induces a series of structural transitions in monodendron molecular self-assembly from lamellar to quadrangular to hexagonal. *Chem. Eur. J.* **15**, 9669–9673. (doi:10.1002/chem.200901618)
29. Katsonis N. 2008 Emerging solvent-induced homochirality by the confinement of achiral molecules against a solid surface. *Angew. Chem. Int. Ed.* **47**, 4997–5001. (doi:10.1002/anie.200800255)
30. Lei S, Tahara K, De Schryver FC, van der Auweraer M, Tobe Y, De Feyter S. 2008 One building block, two different supramolecular surface-confined patterns: concentration in control at the solid–liquid interface. *Angew. Chem. Int. Ed.* **47**, 2964–2968. (doi:10.1002/anie.200705322)
31. Tahara K, Okuhata S, Adisoejoso J, Lei S, Fujita T, De Feyter S, Tobe Y. 2009 2D networks of rhombic-shaped fused dehydrobenzo[12]annulenes: structural variations under concentration control. *J. Am. Chem. Soc.* **131**, 17 583–17 590. (doi:10.1021/ja904481j)
32. Thi Ngoc Ha N, Gopakumar TG, Hietschold M. 2011 Polymorphism driven by concentration at the solid–liquid interface. *J. Phys. Chem. C* **115**, 21 743–21 749. (doi:10.1021/jp111640t)
33. Meier C, Roos M, Künzel D, Breitruck A, Hoster HE, Landfester K, Gross A, Behm RJR, Ziener U. 2009 Concentration and coverage dependent adlayer structures: from two-dimensional networks to rotation in a bearing. *J. Phys. Chem. C* **114**, 1268–1277. (doi:10.1021/jp910029z)
34. Ahn S, Matzger AJ. 2010 Six different assemblies from one building block: two-dimensional crystallization of an amide amphiphile. *J. Am. Chem. Soc.* **132**, 11 364–11 371. (doi:10.1021/ja105039s)
35. Wang Y *et al.* 2012 Varying molecular interactions by coverage in supramolecular surface chemistry. *Chem. Commun.* **48**, 534–536. (doi:10.1039/c1cc14497a)
36. Klappenberger F. 2008 Does the surface matter? Hydrogen-bonded chain formation of an oxalic amide derivative in a two- and three-dimensional environment. *Chemphyschem* **9**, 2522–2530. (doi:10.1002/cphc.200800590)
37. Katsonis N, Marchenko A, Fichou D. 2003 Substrate-induced pairing in 2,3,6,7,10,11-hexakis-undecalkoxy-triphenylene self-assembled monolayers on Au(111). *J. Am. Chem. Soc.* **125**, 13 682–13 683. (doi:10.1021/ja0375737)
38. Kudernac T, Sändig N, Fernández Landaluce T, Van Wees BJ, Rudolf P, Katsonis N, Zerbetto F, Feringa BL. 2009 Intermolecular repulsion through interfacial attraction: toward engineering of polymorphs. *J. Am. Chem. Soc.* **131**, 15 655–15 659. (doi:10.1021/ja901718q)
39. Xie ZX, Xu X, Mao BW, Tanaka K. 2002 Self-assembled binary monolayers of n-alkanes on reconstructed Au(111) and HOPG surfaces. *Langmuir* **18**, 3113–3116. (doi:10.1021/la010869a)
40. Balandina T, Tahara K, Sändig N, Blunt MO, Adisoejoso J, Lei S, Zerbetto F, Tobe Y, De Feyter S. 2012 Role of substrate in directing the self-assembly of multicomponent supramolecular networks at the liquid–solid interface. *ACS Nano* **6**, 8381–8389. (doi:10.1021/nn303144r)
41. Baris B, Luzet V, Duverger E, Sonnet P, Palmino F, Cherioux F. 2011 Robust and open tailored supramolecular networks controlled by the template effect of a silicon surface. *Angew. Chem. Int. Ed.* **50**, 4094–4098. (doi:10.1002/anie.201100332)
42. Marie C, Silly F, Tortech L, Müllen K, Fichou D. 2010 Tuning the packing density of 2D supramolecular self-assemblies at the solid-liquid interface using variable temperature. *ACS Nano* **4**, 1288–1292. (doi:10.1021/nn901717k)
43. Kong X-H, Deng K, Yang Y-L, Zeng Q-D, Wang C. 2007 Effect of thermal annealing on hydrogen bond configurations of host lattice revealed in VOPc/TCDB host-guest architectures. *J. Phys. Chem. C* **111**, 9235–9239. (doi:10.1021/jp070328f)
44. English WA, Hipps KW. 2008 Stability of a surface adlayer at elevated temperature: coronene and heptanoic acid on Au(111). *J. Phys. Chem. C* **112**, 2026–2031. (doi:10.1021/jp076642r)
45. Gutzler R, Sirtl T, Dienstmaier JRF, Mahata K, Heckl WM, Schmittel M, Lackinger M. 2010 Reversible phase transitions in self-assembled monolayers at the liquid-solid interface: temperature-controlled opening and closing of nanopores. *J. Am. Chem. Soc.* **132**, 5084–5090. (doi:10.1021/ja908919r)
46. Bellec A, Arrigoni C, Schull G, Douillard L, Fiorini-Debuisschert C, Mathevet F, Kreher D, Attias A-J, Charra F. 2011 Solution-growth kinetics and thermodynamics of nanoporous self-assembled molecular monolayers. *J. Chem. Phys.* **134**, 124 702–124 707. (doi:10.1063/1.3569132)
47. Kühnle A. 2009 Self-assembly of organic molecules at metal surfaces. *Curr. Opin. Colloid Int.* **14**, 157–168. (doi:10.1016/j.cocis.2008.01.001)

48. Barth JV, Costantini G, Kern K. 2005 Engineering atomic and molecular nanostructures at surfaces. *Nature* **437**, 671–679. (doi:10.1038/nature04166)
49. Gutzler R, Cardenas L, Rosei F. 2011 Kinetics and thermodynamics in surface-confined molecular self-assembly. *Chem. Sci.* **2**, 2290–2300. (doi:10.1039/C1SC00531F)
50. Ilan B, Florio GM, Hybertsen MS, Berne BJ, Flynn GW. 2008 Scanning tunneling microscopy images of alkane derivatives on graphite: role of electronic effects. *Nano Lett.* **8**, 3160–3165. (doi:10.1021/nl8014186)
51. Gong J-R, Wan L-J, Yuan Q-H, Bai C-L, Jude H, Stang PJ. 2005 Mesoscopic self-organization of a self-assembled supramolecular rectangle on highly oriented pyrolytic graphite and Au(111) surfaces. *Proc. Natl Acad. Sci. USA* **102**, 971–974. (doi:10.1073/pnas.0409145102)
52. Tahara K, Yamaga H, Ghijsens E, Inukai K, Adisoejoso J, Blunt MO, De Feyter S, Tobe Y. 2011 Control and induction of surface-confined homochiral porous molecular networks. *Nat. Chem.* **3**, 714–719. (doi:10.1038/nchem.1111)
53. Askadskaya L, Rabe JP. 1992 Anisotropic molecular dynamics in the vicinity of order–disorder transitions in organic monolayers. *Phys. Rev. Lett.* **69**, 1395–1398. (doi:10.1103/PhysRevLett.69.1395)
54. Mammen M, Shakhnovich EI, Whitesides GM. 1998 Using a convenient, quantitative model for torsional entropy to establish qualitative trends for molecular processes that restrict conformational freedom. *J. Org. Chem.* **63**, 3168–3175. (doi:10.1021/jo970943n)
55. Shen Y-T, Deng K, Zhang X-M, Feng W, Zeng Q-D, Wang C, Gong JR. 2011 Switchable ternary nanoporous supramolecular network on photo-regulation. *Nano Lett.* **11**, 3245–3250. (doi:10.1021/nl201504x)
56. Comstock MJ *et al.* 2007 Reversible photomechanical switching of individual engineered molecules at a metallic surface. *Phys. Rev. Lett.* **99**, 038301. (doi:10.1103/PhysRevLett.99.038301)
57. Pace G, Ferri V, Grave C, Elbing M, Von Hänisch C, Zharnikov M, Mayor M, Rampi MA, Samorì P. 2007 Cooperative light-induced molecular movements of highly ordered azobenzene self-assembled monolayers. *Proc. Natl Acad. Sci. USA* **104**, 9937–9942. (doi:10.1073/pnas.0703748104)
58. Elemans JAAW, Lensen MC, Gerritsen JW, Van Kempen H, Speller S, Nolte RJM, Rowan AE. 2003 Scanning probe studies of porphyrin assemblies and their supramolecular manipulation at a solid–liquid interface. *Adv. Mater.* **15**, 2070–2073. (doi:10.1002/adma.200305602)
59. Li Z, Han B, Wan LJ, Wandlowski T. 2005 Supramolecular nanostructures of 1,3,5-benzene-tricarboxylic acid at electrified Au(111)/0.05 M H_2SO_4 interfaces: an in situ scanning tunneling microscopy study. *Langmuir* **21**, 6915–6928. (doi:10.1021/la0507737)
60. Ahn S, Matzger AJ. 2012 Additive perturbed molecular assembly in two-dimensional crystals: differentiating kinetic and thermodynamic pathways. *J. Am. Chem. Soc.* **134**, 3208–3214. (doi:10.1021/ja210933 h)
61. Ciesielski A, Lena S, Masiero S, Spada GP, Samorì P. 2010 Dynamers at the solid–liquid interface: controlling the reversible assembly/reassembly process between two highly ordered supramolecular guanine motifs. *Angew. Chem. Int. Ed.* **49**, 1963–1966. (doi:10.1002/anie.200905827)
62. Li Y, Wan J, Deng K, Han X, Lei S, Yang Y, Zheng Q, Zeng Q, Wang C. 2011 Transformation of self-assembled structure by the addition of active reactant. *J. Phys. Chem. C* **115**, 6540–6544. (doi:10.1021/jp1097876)
63. Merz L, Parschau M, Zoppi L, Baldridge KK, Siegel JS, Ernst K-H. 2009 Reversible phase transitions in a buckybowl monolayer. *Angew. Chem. Int. Ed.* **48**, 1966–1969. (doi:10.1002/anie.200804563)
64. Friesen BA, Bhattarai A, Mazur U, Hipps KW. 2012 Single molecule imaging of oxygenation of cobalt octaethylporphyrin at the solution/solid interface: thermodynamics from microscopy. *J. Am. Chem. Soc.* **134**, 14 897–14 904. (doi:10.1021/ja304431b)
65. Hulsken B *et al.* 2007 Real-time single-molecule imaging of oxidation catalysis at a liquid-solid interface. *Nat. Nanotechnol.* **2**, 285–289. (doi:10.1038/nnano.2007.106)
66. Lackinger M, Heckl WM. 2011 A STM perspective on covalent intermolecular coupling reactions on surfaces. *J. Phys. D: App. Phys.* **44**, 464011. (doi:10.1088/0022-3727/44/46/464011)
67. Perepichka DF, Rosei F. 2009 Extending polymer conjugation into the second dimension. *Science* **323**, 216–217. (doi:10.1126/science.1165429)

68. Tanoue R, Higuchi R, Enoki N, Miyasato Y, Uemura S, Kimizuka N, Stieg AZ, Gimzewski JK, Kunitake M. 2011 Thermodynamically controlled self-assembly of covalent nanoarchitectures in aqueous solution. *ACS Nano* **5**, 3923–3929. (doi:10.1021/nn200393q)
69. Dienstmaier JF, Gigler AM, Goetz AJ, Knochel P, Bein T, Lyapin A, Reichlmaier S, Heckl WM, Lackinger M. 2011 Synthesis of well-ordered COF monolayers: surface growth of nanocrystalline precursors versus direct on-surface polycondensation. *ACS Nano* **5**, 9737–9745. (doi:10.1021/nn2032616)
70. Dienstmaier JF, Medina DD, Dogru M, Knochel P, Bein T, Heckl WM, Lackinger M. 2012 Isoreticular two-dimensional covalent organic frameworks synthesized by on-surface condensation of diboronic acids. *ACS Nano* **6**, 7234–7242. (doi:10.1021/nn302363d)